

Article

“Free of Base” Sulfa-Michael Addition for Novel *o*-Carboranyl-DL-Cysteine Synthesis †

Julia Laskova ^{1,*}, Irina Kosenko ¹, Ivan Ananyev ¹, Marina Stogniy ^{1,2}, Igor Sivaev ¹ 
and Vladimir Bregadze ¹

¹ A.N.Nesmeyanov Institute of Organoelement Compounds, Russian Academy of Sciences, Vavilova str. 28, 119991 Moscow, Russia; ira.kosenko@gmail.com (I.K.); i.ananyev@gmail.com (I.A.); stogniyarina@rambler.ru (M.S.); sivaev@ineos.ac.ru (I.S.); bre@ineos.ac.ru (V.B.)

² M.V. Lomonosov Institute of Fine Chemical Technology, MIREA—Russian Technological University, 86 Vernadsky Av., 119571 Moscow, Russia

* Correspondence: laskova@ineos.ac.ru; Tel.: +7-905-551-8846

† Dedicated to Professor Alan J. Welch in recognition of his outstanding contribution in the chemistry of carboranes.

Received: 2 November 2020; Accepted: 7 December 2020; Published: 11 December 2020



Abstract: The sulfa-Michael addition reaction was applied for the two-step synthesis of *o*-carboranyl cysteine 1-HOOCCH(NH₂)CH₂S-1,2-C₂B₁₀H₁₁ from the trimethylammonium salt of 1-mercapto-*o*-carborane and methyl 2-acetamidoacrylate. To avoid the decapitation of *o*-carborane into its *nido*-form, the “free of base” method under mild conditions in a system of two immiscible solvents toluene-H₂O was developed. The replacement of H₂O by ²H₂O resulted in carboranyl-cysteine containing a deuterium label at the α-position of the amino acid 1-HOOCCHD(NH₂)CH₂S-1,2-C₂B₁₀H₁₁. The structure of the protected *o*-carboranyl cysteine was determined by single-crystal X-ray diffraction. The obtained compounds can be considered as potential agents for the Boron Neutron Capture Therapy of cancer.

Keywords: boron chemistry; *o*-carborane; sulfa-Michael addition reaction; cysteine; boron neutron capture therapy; *o*-carborane decapitation; labeled compound

1. Introduction

Cancer remains one of the major health issues and the second leading cause of death worldwide [1]. Radiation therapy has a central role in the management of malignant brain tumors, especially for the most aggressive ones [2–4]. First introduced in 1936 by Locher [5], the Boron Neutron Capture Therapy model (BNCT) is a promising type of radiation therapy for cancer that has the potential to be an important treatment for numerous types of tumors, including for those lying in areas that are difficult to access for surgery intervention, such as high-grade gliomas and metastatic brain tumors [6–8]. Currently, only two low molecular weight boron-containing compounds, sodium mercapto-undecahydro-*closo*-dodecaborate (BSH, developed in about 1965) and a water-soluble fructose complex of borylphenylalanine (BPA, discovered in 1958), have been approved and found clinical use in BNCT [9–11].

Recent advances in the development of potential agents for BNCT treatment include various boron-containing bioconjugates [12]; there are many with natural and unnatural amino acids among them [13]. It is believed that amino acid conjugates are preferentially taken up by rapidly growing tumor cells [14]. Polyhedral carboranes as a boron-rich compounds are considered to have potential for usage in BNCT [15]. In this regard, the chemistry of dicarbaboranes [C₂B₁₀H₁₂] and their derivatives has been well investigated [16]. The synthesis of *o*-carboranes containing unnatural ω-mercapto-amino

acids with side-chain lengths ranging from 4 to 6 methylene units **1(a–c)** [17], *L*-*o*-carboranyl-alanine **2** [18] as well as *o*-carboranyl derivatives of (S)-Asparagine **3a** and (S)-Glutamine **3b** [19], phenylalanine **4** [20] and (S)-*m*-carboranyl-homocysteine sulfoxide **5** [21], have been published. Our current interest was inspired by the recent synthesis [22] of *m*-carboranyl-cysteine **6** and its biological evaluation as an agent for Boron Neutron Capture Therapy [23,24] (Figure 1). Therefore, we decided to synthesize its analogue based on readily available 1-mercapto-*o*-carborane [25,26].

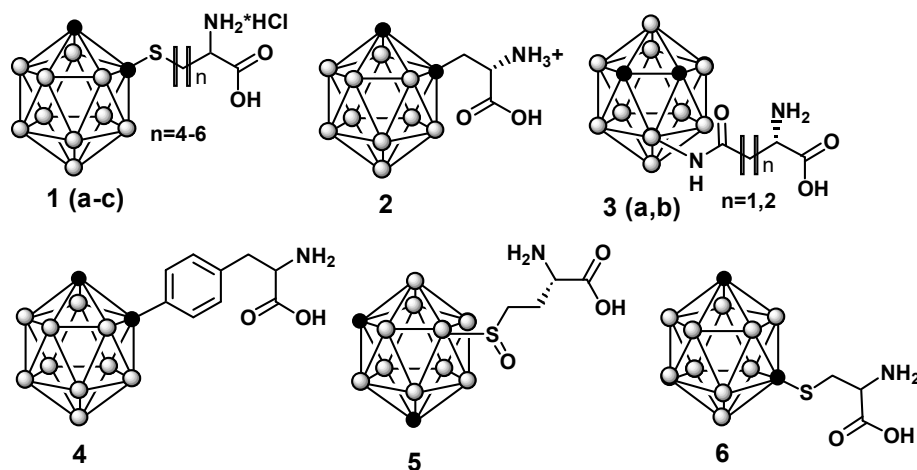


Figure 1. *o*- and *m*- carborane–amino acid conjugates.

Here, we report the synthesis of *o*-carboranyl-cysteine via the sulfa-Michael addition reaction of an easily available salt of 1-mercapto-*o*-carborane and methyl 2-acetamidoacrylate (MAA) using a two-phase system.

2. Materials and Methods

2.1. General

[1-*S*-1,2- $C_2B_{10}H_{11}$](Me_3NH) (**7**) was prepared according to the literature procedure [27]. Methyl 2-acetamidoacrylate (Sigma Aldrich Chemie GmbH, NJ, USA) was used without purification. 2H_2O was received from Carl Roth GmbH. The reaction proceedings were monitored via thin-layer chromatograms (Merck F254 silica gel on aluminum plates). Boron compounds were visualized with $PdCl_2$ stain solution, which, upon heating, gave dark brown spots. Purifications were carried out using column chromatography with Silica gel 60 0.060–0.200 mm (Acros Organics, NJ, USA). 1H , ^{13}C , and ^{11}B NMR spectra were recorded at 400.13, 100.61, and 128.38 MHz, respectively, on a BRUKER-Avance-400 spectrometer. Tetramethylsilane and $BF_3 \times Et_2O$ were used as standards for 1H , ^{13}C NMR, and ^{11}B NMR, respectively. All the chemical shifts are reported in ppm (δ) relative to external standards. IR spectra were recorded on an IR Prestige-21 (SHIMADZU, Kyoto, Japan) instrument. High-resolution mass spectra (HRMS) were measured on a Bruker micrOTOF II instrument using electrospray ionization (ESI), with a mass range from m/z 50 to m/z 3000; external or internal calibration was carried out with ESI Tuning Mix, Agilent. Spectra can be found in the Supplementary Materials.

2.2. Synthesis of 1- $CH_3O(O)C(CH_3(O)CHN)CHCH_2S$ -1,2- $C_2B_{10}H_{11}$ (**8**)

To a solution of **7** (0.5 g, 2.1 mmol) in toluene (30 mL) methyl 2-acetamidoacrylate (0.3 g, 2.1 mmol) and H_2O (30 mL) were added; the resulting system was vigorously stirred under reflux for 24 h. Then, the mixture was cooled to r.t. and the toluene layer was separated, washed with H_2O (2×20), dried over Na_2SO_4 , and evaporated. The product was purified by silica gel column chromatography using Et_2O as an eluent and vacuum-dried to give a light yellow solid. Yield: 0.46 g (68%). 1H NMR (Chloroform- d) δ = 6.29 (d, J = 7.7 Hz, 1H, NH), 4.89 (td, J = 7.2, 4.5 Hz, 1H, α -CH), 3.99 (broad

s, 1H, carb-CH), 3.82 (s, 3H, COOCH₃), 3.51 (dd, *J* = 13.4, 4.6 Hz, 1H, CH₂CH), 3.18 (dd, *J* = 13.4, 6.9 Hz, 1H, CH₂CH), 2.06 (s, 3H, NHCOCH₃), 3.0–1.5 (broad, 10H, BH); ¹¹B NMR (Chloroform-*d*) δ = −1.5 (d, *J* = 150 Hz, 1B), −4.7 (d, *J* = 146 Hz, 1B), −8.8 (d, *J* = 154 Hz, 4B), −12.2 (d, *J* = 162 Hz, 4B); ¹³C NMR (Chloroform-*d*) δ = 170.21, 170.17 (CO), 73.9, 67.9 (C-carb), 53.2 (OCH₃), 51.2 (α-CH), 39.4 (CH₂CH), 23.1 (COCH₃). ESI-MS, *m/z*, C₈H₂₁B₁₀NO₃S calcd. 320.2322, found 320.2322 ([M+H]⁺). IR-FT (ν, cm^{−1}): 3371(NH), 3060 (CH-carb); 2948, 2926, 2852 (broad CH); 2607, 2584, 2557 (BH); 1736, 16177 (CO).

2.3. Synthesis of 1-HOOC(NH₂)CHCH₂S-1,2-C₂B₁₀H₁₁ × HCl (**9**)

Water (2 mL) and concentrated HCl (10 mL) were added to a solution of **8** (0.1 g, 0.3 mmol) in glacial acetic acid (10 mL). The resulting mixture was heated at 70 °C for 40 h., cooled to r.t., and evaporated. The residue was suspended in 5 mL of water, formed solid was filtered, washed with water (2 × 5 mL) and vacuum dried to give **9**. Light yellow solid (0.093 mg, 70%). ¹H NMR (Methanol-*d*₄) δ = 4.89 (s, 1H, carb-CH), 4.09 (m, 1H, α-CH), 3.64 (m, 1H, CH₂CH), 3.43 (m, 1H, CH₂CH), 3.0–1.5 (broad, 10H, BH); ¹¹B NMR (Methanol-*d*₄) δ = −1.8 (d, *J* = 151 Hz, 1B), −5.1 (d, *J* = 148 Hz, 1B), −9.2 (d, *J* = 148 Hz, 4B), −12.3 (d, *J* = 172 Hz, 4B). ¹³C NMR (Methanol-*d*₄) δ 172.0 (COOH), 74.8, 68.4 (C-carb), 51.60 (α-CH), 38.3 (CH₂CH). ESI-MS, *m/z*, C₅H₁₇B₁₀NO₂S calcd. 264.2059, found 264.2061. IR-FT (ν, cm^{−1}): 3399 (broad NH⁺), 3058 (CH- carb); 2923, 2854 (CH); 2580 (broad BH), 1728 (CO).

2.4. Synthesis of 1-CH₃O(O)C(CH₃(O)CHN)CDCH₂S-1,2-C₂B₁₀H₁₁ (**10**)

Under an argon atmosphere, methyl 2-acetamidoacrylate (0.06 g, 0.4 mmol) and ²H₂O (5 mL) were added to a solution of **7** (0.1 g, 0.4 mmol) in toluene (15 mL); the resulting two-phase system was vigorously stirred under reflux for 30 h. Purification was held in the same manner as for compound **8**. Light yellow solid (90 mg, 66%). ¹H NMR (Chloroform-*d*) δ = 6.31 (s, 1H, NH), 4.00 (broad s, 1H, CH-carb), 3.82 (s, 3H, COOCH₃), 3.50 (d, *J* = 13.4 Hz, 1H, CH₂CD), 3.17 (d, *J* = 13.4 Hz, 1H, CH₂CD), 2.06 (s, 3H, NHCOCH₃), 3.0–1.5 (broad, 10H, BH); ¹¹B NMR (Chloroform-*d*) δ = −1.5 (d, *J* = 151 Hz, 1B), −4.8 (d, *J* = 150 Hz, 1B), −8.9 (d, *J* = 151 Hz, 4B), −12.4 (d, *J* = 176 Hz, 4B); ¹³C NMR (Chloroform-*d*) δ = 170.23, 170.17 (CO), 73.9, 67.9 (C-carb), 53.2 (OCH₃), 51.0 (t, α-CD), 39.3 (CH₂), 23.1 (COCH₃). ESI-MS, *m/z*, C₈H₂₀DB₁₀NO₃S calcd. 321.2385, found 321.2399. IR-FT (ν, cm^{−1}): 3370 (NH), 3061 (CH- carb); 2953 (CH); 2608, 2586, 2557 (BH), 1733, 1674 (CO).

2.5. Synthesis of 1-HOOC(NH₂)CDCH₂S-1,2-C₂B₁₀H₁₁ × HCl (**11**)

Water (2 mL) and concentrated HCl (5 mL) were added to a solution of **10** (0.05 g, 0.16 mmol) in glacial acetic acid (5 mL). The resulting mixture was heated at 70 °C for 40 h., cooled to r.t., and evaporated. The residue was suspended in 5 mL of water, formed solid was filtered, washed with water (2 mL) and vacuum dried to yield **11**: 38 mg (81%). ¹H NMR (Methanol-*d*₄) δ = 4.88 (broad s, 1H, CH-carb), 4.27–4.20 (α-CH, m, 0,1H), 3.64 (d, *J* = 13.9 Hz, 1H, CH₂CD), 3.44 (d, *J* = 13.9 Hz, 1H, CH₂CD), 3.0–1.5 (broad, 10H, BH). ¹¹B NMR (Methanol-*d*₄) δ = −1.9 (d, *J* = 149 Hz, 1B), −4.9 (d, *J* = 140 Hz, 1B), −9.0 (d, *J* = 143 Hz, 4B), −12.3 (d, *J* = 175 Hz, 4B). ¹³C NMR (Methanol-*d*₄) δ = 168.0 (CO), 73.6 (C-carb), 68.4 (C-carb), 51.8 (α-C), 36.0 (CH₂). ESI-MS, *m/z*, C₅H₁₇B₁₀NO₂S calcd. 265.2122, found 265.2127.

2.6. Synthesis of 1-CH₃O(O)C(CH₃(O)CHN)CHCH₂S-2-D-1,2-C₂B₁₀H₁₀ (**12**)

Under an argon atmosphere, methyl 2-acetamidoacrylate (0.06 g, 0.4 mmol), ²H₂O (5 mL), and anhydrous K₂CO₃ (0.055 g, 0.4 mmol) were added to a solution of **7** (0.1 g, 0.4 mmol) in toluene (15 mL); the resulting system was vigorously stirred under reflux for 10 h. The purification was held in the same manner as for compound **8**. Light yellow solid (13 mg, 10%). ¹H NMR (Chloroform-*d*) δ = 6.20 (d, *J* = 7.7 Hz, 1H, NH), 4.90 (td, *J* = 7.2, 4.7 Hz, 1H, α-CH), 4.00 (undetectable, s, 0H, carb-CD), 3.83 (s, 3H, COOCH₃), 3.53 (dd, *J* = 13.4, 4.7 Hz, 1H, CH₂CH), 3.19 (dd, *J* = 13.4, 6.9 Hz, 1H, CH₂CH), 2.07 (s, 3H, NHCOCH₃), 3.0–1.5 (broad, 10H, BH); ¹¹B NMR (Chloroform-*d*) δ = −1.5 (d, *J* = 152 Hz, 1B), −4.8 (d, *J* = 147 Hz, 1B), −8.9 (d, *J* = 152 Hz, 4B), −12.5 (d, *J* = 173 Hz, 4B); ¹³C

NMR (Chloroform-*d*) δ = 170.16, 170.14 (CO), 73.8 (CH-carb), 68.5–66.8 (t, CD-carb), 53.2 (OCH₃), 51.2 (α -CH), 39.4 (CH₂), 23.1 (COCH₃). ESI-MS, *m/z*, C₈H₂₀DB₁₀NO₃S calcd. 321.2385, found 321.2384. IR-FT (ν , cm⁻¹): 3372(NH), 2923, 2851 (CH); 2607, 2584, 2557 (BH); 2289 (CD-carb); 1736, 1677 (CO).

2.7. X-ray Diffraction

Crystals of **8** are triclinic, space group P-1, at 120K: *a* = 7.6513(5), *b* = 10.5669(7), *c* = 11.5392(7), α = 68.378(1)°, β = 85.686(1)°, γ = 72.663(1)°, *V* = 827.27(9) Å³, *Z* = 2 (*Z'* = 1), *d*_{calc} = 1.282 g·cm⁻³, *F*(000) = 332. Intensities of 11,058 reflections were measured with a Bruker SMART APEX 2 Duo CCD diffractometer [λ (MoK α) = 0.71072 Å, ω -scans, $2\theta < 60^\circ$] and 4824 independent reflections [*R*_{int} = 0.0324] were used in further refinement. The structure was solved by the direct method and refined by the full-matrix least-squares technique against *F*² in the anisotropic-isotropic approximation. The hydrogen atoms were found in the difference Fourier synthesis and refined in the isotropic approximation within the riding model. For **8**, the refinement converged to *wR*₂ = 0.1167 and GOF = 0.781 for all independent reflections (*R*₁ = 0.0371 was calculated for 3661 observed reflections with *I* > 2 σ (*I*)). All the calculations were performed using SHELX2018 [28]. The CCDC 2034871 contains the supplementary crystallographic data for **8**. These data can be obtained free of charge via <http://www.ccdc.cam.ac.uk/conts/retrieving.html> (or from the CCDC, 12 Union Road, Cambridge, CB21EZ, UK; or deposit@ccdc.cam.ac.uk).

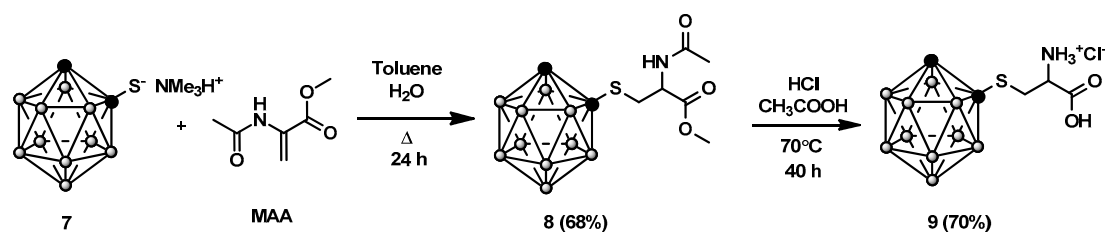
Computational details: All the calculations were conducted in the Gaussian09 program (rev. D01) [28]. The geometry optimization procedures were performed using standard criteria on displacements and forces. The DFT optimization were performed using the PBE0 functional [29,30] and the 6-311++G(d,p) basis set (ultrafine integration grids were used). The non-specific solvation was modelled using the self-consistent reaction field approach (PCM model, ϵ = 72). The influence of specific solvation on the geometry of **8** was accounted for by the optimization of a central molecule in clusters; two models were used: (1) the trimer of molecules from crystal of **8** with fixed coordinates and normalized X-H bond lengths for lateral molecules and (2) the shell of molecules from crystal of **8** with fixed coordinates and normalized X-H bond lengths. The Quantum theory of Atoms in Molecules surface integrals for the trimer were calculated using the AIMAll program [31]. The shell in the second model was generated using the criteria of at least one geometrical contact (within the sum of van der Waals radii plus 5 Å) between the surrounding molecules and the central molecule. The shell was described by the ONIOM approach (PBE0/6-311++G(d,p):PBE0/3-21G), and only the internal layer (the central molecule) was optimized. The Hessian calculations for all the optimized structures revealed their correspondence to energy minimums.

3. Results

3.1. *o*-Carboranyl-Cysteine Synthesis

The reaction conditions for the sulfa-Michael addition of thiophenols to methyl 2-acetamidoacrylate are well-studied [32]. It has been shown that reactions proceed in toluene or THF with catalytic quantity of the basic salt K₂CO₃ in the presence of solid-liquid phase-transfer catalyst. On the one hand, it was reasonable to apply conditions studied for thiophenols to the mercapto derivative of *o*-carborane; however, prolonged reaction with a base may cause of a side reaction due to the well-known property of *o*-carborane to undergo deboronation in the presence of bases, even mild ones, to yield *nido*-[7,9-C₂B₉H₁₂] [33–39]. The deboronation of *o*-C₂B₁₀H₁₂ proceeds fairly easily, whereas *m*-C₂B₁₀H₁₂, which was used for the synthesis of **6**, is much more stable under the same conditions. A detailed study of such differences has been presented [40]. On the other hand, more common work up of *o*-carboranyl thiols includes the conversion of the formed SH-derivative to the more stable triethylammonium [41,42] or trimethylammonium salt [27] **7** (Scheme 1). The usage of the trimethylammonium salt **7** let us to avoid the deprotonation stage during the reaction process to keep the *o*-carborane structure from degradation under the action of a base. The synthetic route developed

for the preparation of the cysteine derivative of *o*-carborane conjugate with cysteine is outlined in Scheme 1.



Scheme 1. Synthesis of *o*-carboranyl cysteine.

Compared to mercapto-*o*-carborane, *o*-carboranyl thiolate **7** lacks sufficient acidic hydrogen, which is necessary for the reaction to proceed. We found that reaction of **7** with methyl 2-acetamidoacrylate in a biphasic toluene-H₂O system under reflux for 24 h without base or any additional catalyst results in the formation of sulfa-Michael addition reaction product **8**.

The structure of **8** was confirmed by ¹H, ¹¹B, ¹³C NMR, and IR spectroscopy, high-resolution mass spectrometry, and single-crystal X-ray diffraction study. The ¹H NMR spectrum of **8** in CDCl₃ shows two singlets at 2.06 and 3.83 due to the acetamide and the ester groups, a doublet at 6.17 ppm from the NH-group, a multiplet at 4.90 ppm attributed to the proton bonded to the α-carbon, two doublets of doublets at 3.51 and 3.18 ppm assigned to the diastereotopic methylene protons, and a broad singlet of carborane C-H group at 3.99 ppm. The ¹³C-NMR spectrum contains signals of two carbonyl groups at 170.21 and 170.17 ppm., two cluster carbons at 73.9 and 67.9 ppm, two methyls of ester at 53.2 and acetamide at 23.1 ppm., as well as the CH and CH₂ groups at 51.2 and 39.4 ppm. The ¹¹B and ¹¹B{¹H} NMR spectra are in agreement with the C-mono-substituted *o*-carborane structure.

The solid-state structure of **8** was determined by single-crystal X-ray diffraction. The molecule of **8** is crystallized as the racemate in the centrosymmetric P-1 space group and contains a stereocenter at the C4 atom (Figure 2).

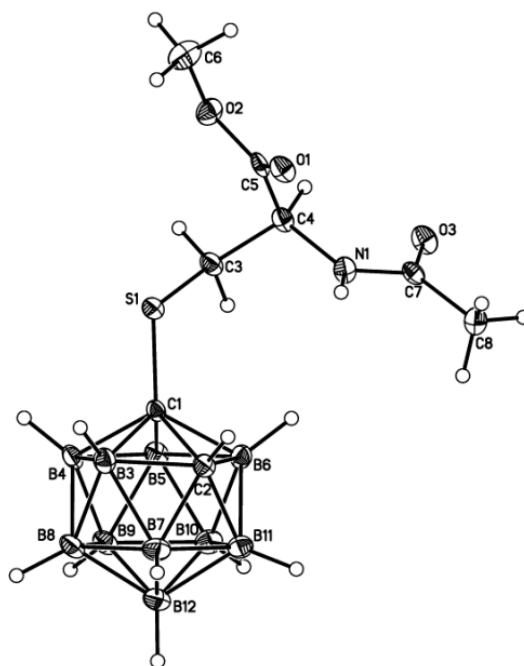


Figure 2. General view of the molecule **8** in crystal. Non-hydrogen atoms are given as probability ellipsoids of atomic displacements ($p = 0.5$).

While the main structural features of **8** are expected for this class of compounds (the C1-C2, S1-C1, and S1-C3 bond lengths equal 1.669(2), 1.791(1), and 1.826(1) Å, respectively; the sum of valence angles at the amide-type N1 atom equals 358.9°), the rotation of the substituent at the C1 atom with respect to the carborane cage can, however, hardly be rationalized by common intramolecular structural effects. For instance, the lone electron pairs of the S1 atom are nearly coplanar to the C3-H and C3-C4 bonds that contradicts the preferred geometry of expected LP(S)→σ* stereoelectronic interactions (Figure 3a). Indeed, the Cambridge Structural Database search reveals the predominance of staggered conformations of the C-S_{sp3}-C_{sp3}-C_{sp3} fragments (Figure 3b), whereas the corresponding torsion angle equals 118.1(2)° in **8**.

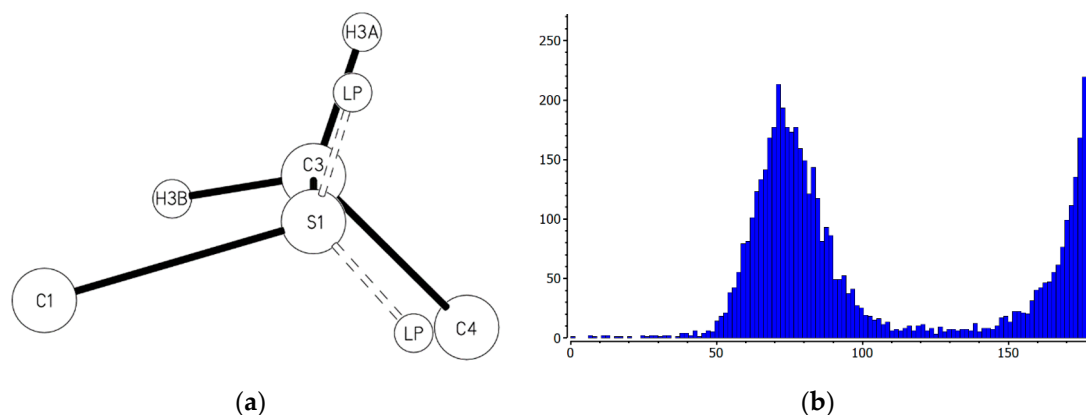


Figure 3. The conformation of the C1-S1-C3-C4 fragment in **8** (LP—positions of lone electronic pairs, (a)) and the distribution of corresponding torsion angles in the C-S_{sp3}-C_{sp3}-C_{sp3} fragments retrieved from the Cambridge Structural Database (b).

Based on the geometrical analysis of the crystal packing of **8**, it has been found that the substituent conformation could be stabilized by the environment effects. Indeed, there are several shortened intermolecular contacts formed by atoms of the C1 substituent which can be attributed to rather strong interactions – NH ... O H-bonds (N1 ... O1 2.933(2) Å, NHO 161.3° with normalized N-H bond length) and O ... π interactions (O1 ... O3 3.020(2) Å), both bounding molecules into infinite chains (Figure 4). The weak BH ... HC and CH ... O interactions are the only meaningful interactions between these chains.

In order to reveal the influence of environment effects on the conformation of **8**, the DFT calculations were additionally performed. Indeed, both the isolated molecule optimization and the optimization of **8** accounting for non-specific solvation effects (the SCRF-PCM model, relative dielectric permittivity of 72) produced structures being significantly different from those observed in the crystal: the root-mean-square deviations of the best overlap for non-hydrogen atoms are 0.495 and 0.446 Å, respectively. Surprisingly, the explicit DFT treatment of three neighboring molecules from a chain (see Figure 4) forming the mentioned shortened intramolecular contacts did not lead to any pronounced changes: the rmsd value for the central molecule in the calculated trimer equals 0.320 Å. Note that the total energy of mentioned N-H ... O H-bonds and O ... π interactions exceeds 24 kcal·mol⁻¹ according to the QTAIM electron density analysis [43] carried out for the trimer. Our best result was achieved by the ONIOM calculation, which considers all neighboring molecules at the DFT level (the rmsd value equals to 0.168 Å, Figure 5). Thus, despite the relatively large strength of the H-bonds and O ... π interactions, the conformation of **8** in crystal depends heavily on the peculiarities of other, weaker intermolecular interactions such as BH ... HC and CH ... O.

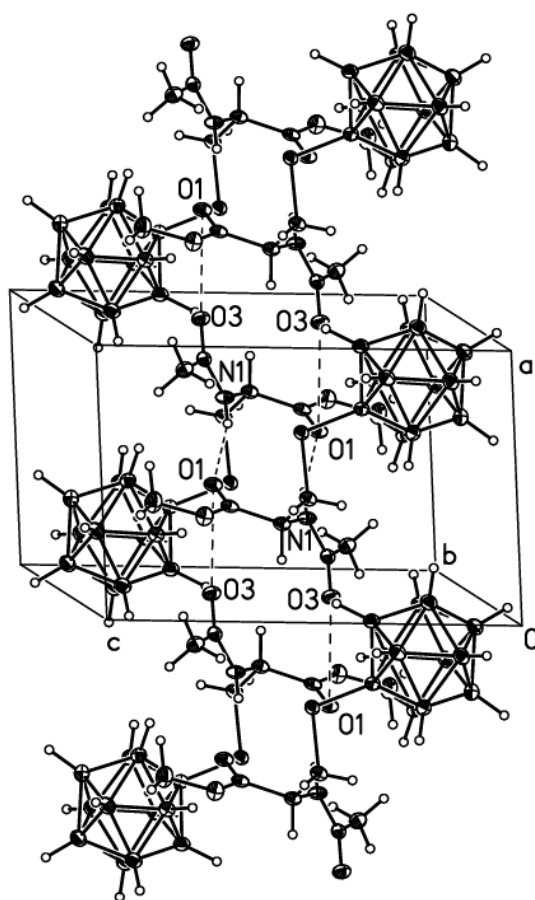


Figure 4. A fragment of the infinite chain formed in crystal of **8** along the *a* axis. Non-hydrogen atoms are given as probability ellipsoids of atomic displacements ($p = 0.5$).

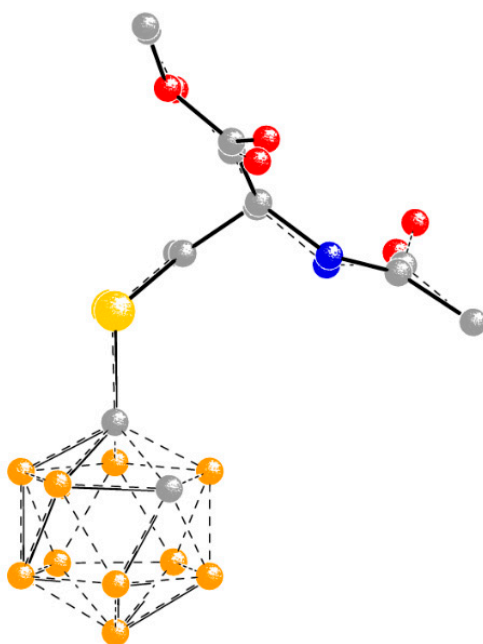
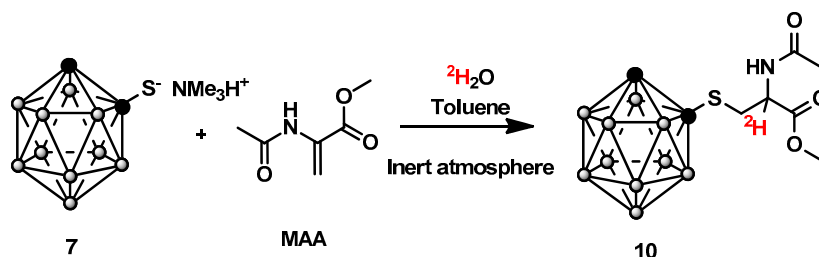


Figure 5. The best root-mean-square overlap for non-hydrogen atoms between crystal (solid lines) and ONIOM-modelled (dashed lines) conformations of **8**.

The treatment of **8** with a mixture of glacial acetic and hydrochloric acids under heating gave the title S-substituted cysteine **9** in the form of hydrochloride with a good yield (Scheme 1). The synthesized amino acid was characterized by ^1H , ^{11}B , ^{13}C NMR spectroscopy, IR spectroscopy, and high-resolution mass spectrometry. A singlet at 4.89 ppm corresponding to the C-H from the o-carborane was observed in the ^1H NMR; other chemical shifts agreeing with amino acid structure were also observed.

3.2. The Sulfa-Michel Addition Mechanism Investigation for o-Carboranyl Cysteine and Synthesis of Deuterium Labeled Compounds

The investigation of the reaction conditions for the synthesis of **8** revealed a crucial role of the choice of solvent. Thus, the formation of only an insignificant amount of **8** was observed when the reaction proceeded in homogenous systems EtOH-H₂O or THF-H₂O, whereas in absolute EtOH no product was detected at all. The best result was achieved when the toluene-H₂O system was used without any base. Since the initial salt **7** did not have an acid proton, as 1-mercapto-o-carborane has, this is why we assumed that α -proton comes into intermediate **8** from water. To gain some insight into the process, we carried out the “free of base” reaction with $^2\text{H}_2\text{O}$, which required strictly anhydrous conditions (Scheme 2).



Scheme 2. Synthesis of the labeled with deuterium o-carboranyl conjugate.

We found that the two-phase system reaction proceeds in the way we proposed. Compound **10** with deuterium at the α -position of amino acid was isolated and characterized by NMR, IR spectroscopy, and mass spectrometry. The reaction time for the synthesis of **10** in the toluene- $^2\text{H}_2\text{O}$ system increased as compared with those in the toluene-H₂O system. This difference in reaction time may be attributed to the presence of a deuterium isotope effect. The yield of reaction, which was detected, remains over 65%. The comparison of the ^1H NMR and ^{13}C spectra of **8** and **10** is displayed below (Figure 6).

The ^1H NMR spectrum of **10** in CDCl₃ does not contain the multiplet at 4.90 ppm, which indicates the absence of a proton at the α -position of the amino acid, whereas in the ^{13}C -NMR spectrum the triplet due to the C²H group appears at 51.0 ppm, indicating the substitution of H for ^2H . In addition, the doublet of the NH group (6.17 ppm) and two doublets of doublets from the methylene CH₂ protons, which were detected in the ^1H NMR spectrum of **8**, collapsed to a singlet and two doublets in the spectrum of [α - ^2H]carboranyl-cysteine **10**, respectively, due to the absence of an adjacent proton.

The subsequent acid hydrolysis of **10** resulted in the o-carboranyl-cysteine **11**, labeled at the α -position of the amino acid (Scheme 3).

The presence of ^2H and its position were determined by high-resolution mass spectrometry and ^1H NMR spectroscopy. The ^1H NMR spectrum showed the presence of an unlabeled compound in an amount of less than 10% (Figure 7).

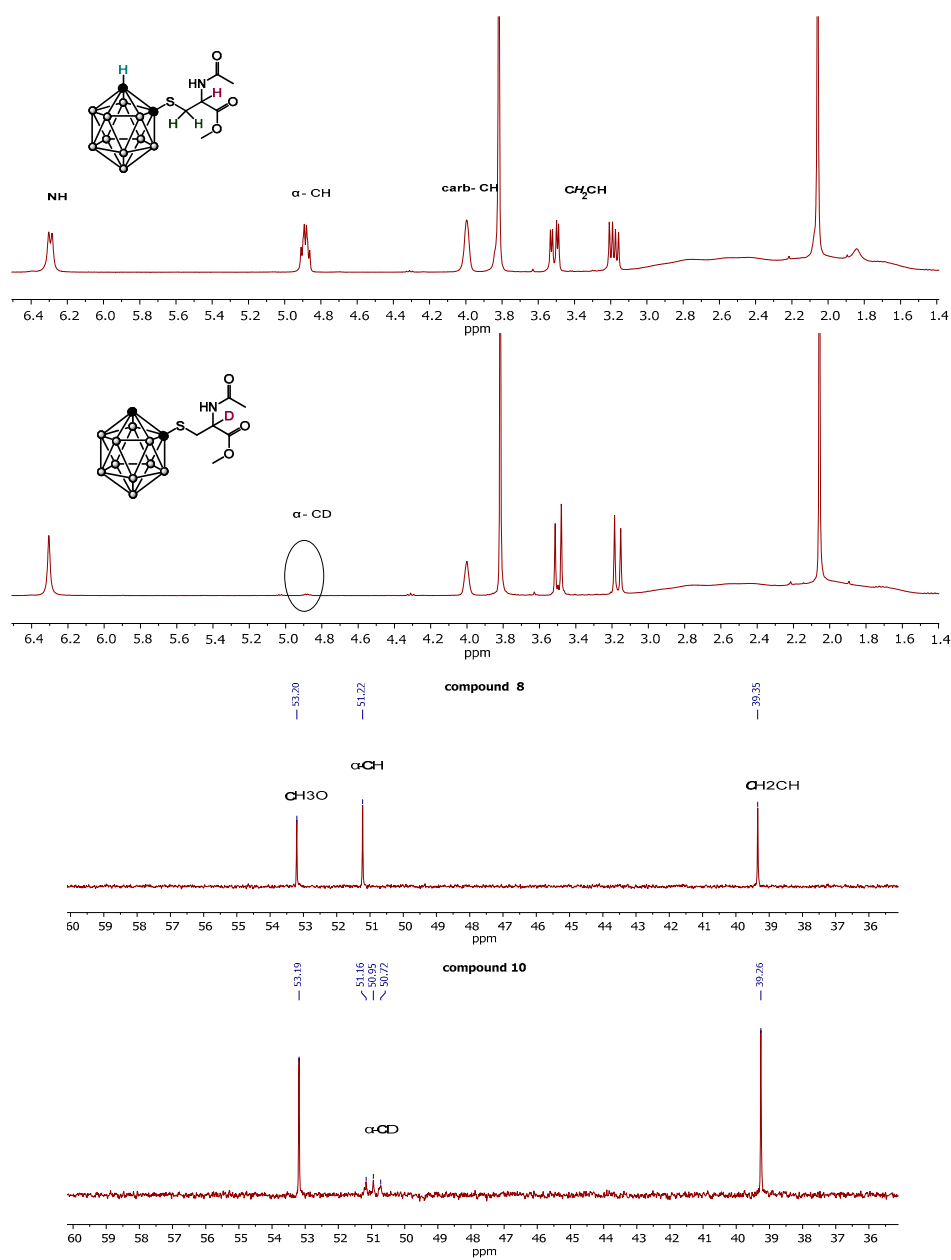
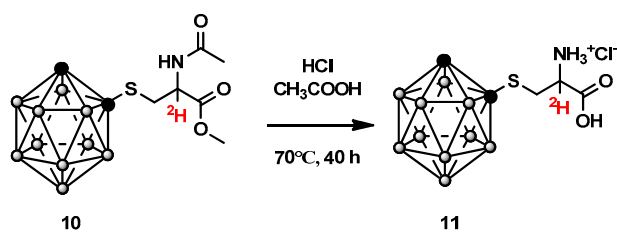


Figure 6. Comparison of ^1H NMR and fragments of the ^{13}C NMR spectra of 8 and 10 in CDCl_3 .



Scheme 3. O-carboranyl-DL-[$\alpha\text{-}^2\text{H}$]-cysteine synthesis.

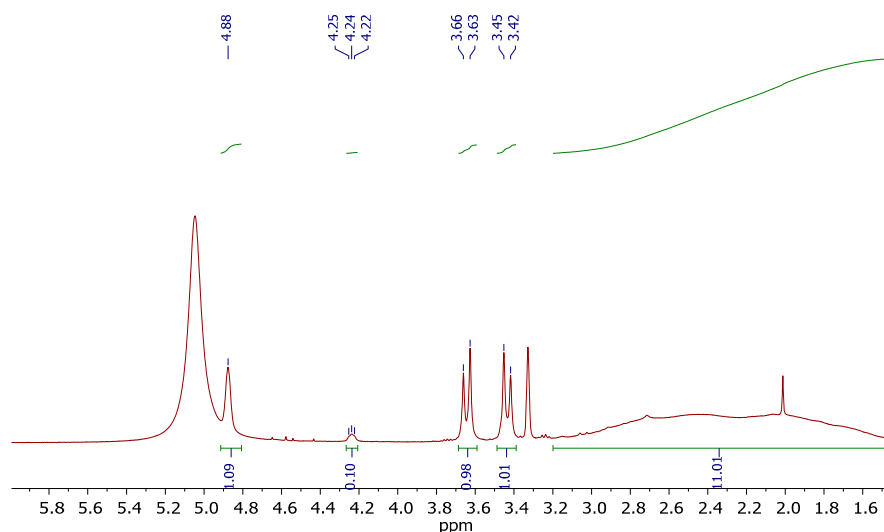
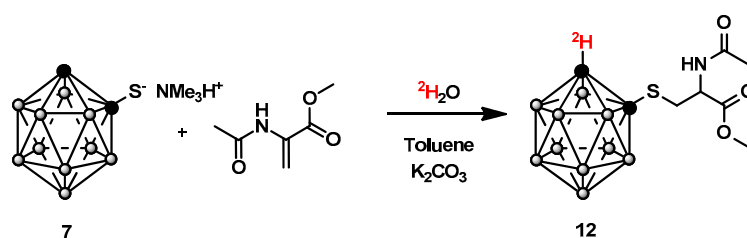


Figure 7. ^1H NMR spectrum of **11** in methanol- d_4 .

The method proposed above can be considered as a preparative one for the synthesis of labeled *o*-carboranyl-DL- $[\alpha\text{-}^2\text{H}]$ -cysteine, which could be useful for study of the metabolism of *o*-carboranyl-DL-cysteine itself, as well as the metabolism of boron-containing proteins on its base as potential BNCT agents [44–46].

It was mentioned that the *o*-carborane system is sensitive to the presence of a base. To investigate the effect of water-soluble basic salt toward the reaction that proceeds in a two-phase system, we added K_2CO_3 to the reaction system. We found that the addition of a basic salt accelerates the reaction, which is complete in 8 h, but resulted in an only 17% yield of **8**, while the main product is *nido*-carborane derivatives, as found by ^{11}B NMR. The solvent change from H_2O to $^2\text{H}_2\text{O}$ along with the use of anhydrous K_2CO_3 and a Schlenk technique under an atmosphere of argon increases the reaction time from 8 h to 10 h due to the isotope effect, and the yield of product falls from 17% to 10%. Interestingly, the structure of the resulting product was found to be different from **8** and **10**. According to the NMR spectroscopy data, deuterium from $^2\text{H}_2\text{O}$ took up a place of the 1-CH-*o*-carborane proton, whereas proton appeared at the α -position of the amino acid (Scheme 4, Figure 8). Compound **12** was isolated and characterized, and its structure and composition were confirmed by ^1H , ^{11}B , ^{13}C NMR, and IR spectroscopy and high-resolution mass spectrometry.



Scheme 4. The sulfa-Michael addition reaction in the presence of the basic salt.

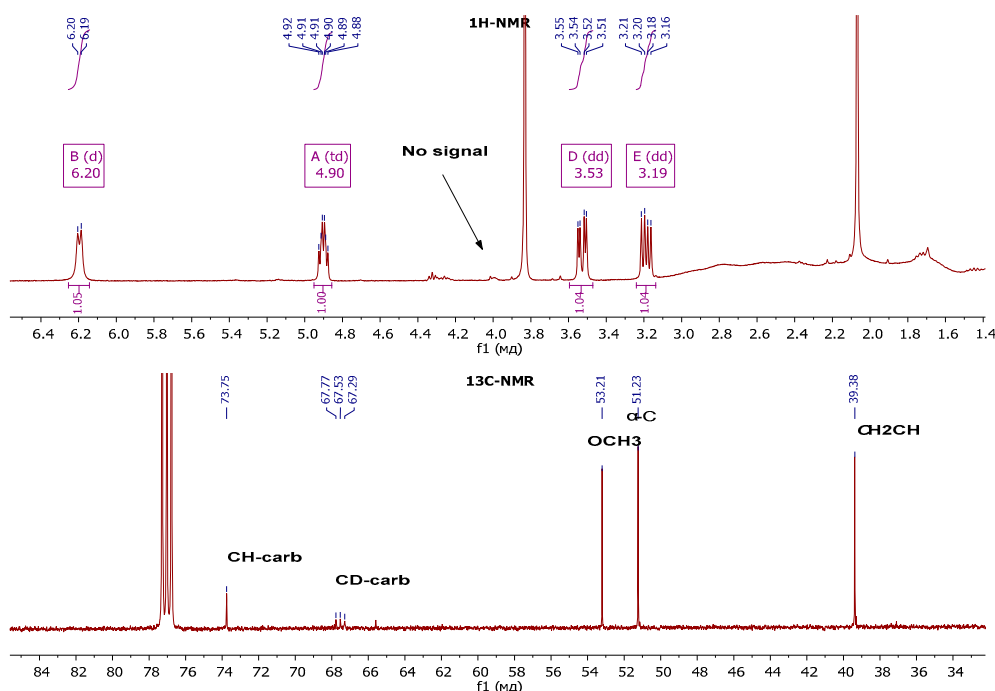
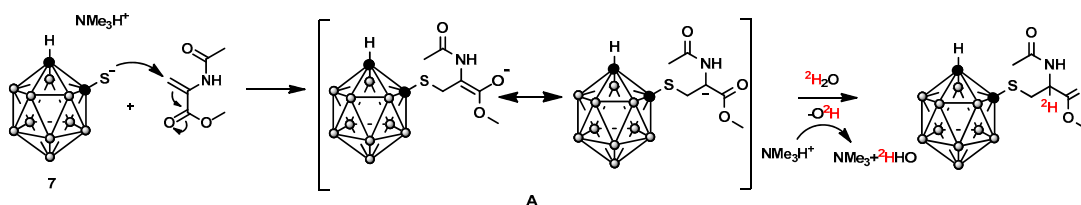


Figure 8. ^1H and a fragment of ^{13}C NMR spectra of **12** in CDCl_3 .

4. Discussion

To summarize the obtained results, we assumed the mechanism of reaction proceeding (Scheme 5).



Scheme 5. Proposed mechanism of the reaction of trimethylammonium salt of 1-mercapto-*o*-carborane with methyl 2-acetamidoacrylate.

The reaction realizes according to a classical Michael addition reaction, where thiolate **7** acts as a nucleophile without additional deprotonation. In the first step, nucleophile reacts with the electrophilic alkene to form **A** in a conjugate addition reaction. In the next stage, the deuterium abstraction from solvent by the enolate **A** forms the final conjugate and a $^2\text{HO}^-$ anion from a water molecule. $^2\text{HO}^-$ anion, being a base, may cause a deboronation process, however its cooperation with a cation forms a water-soluble trimethylammonium hydroxide. When the reaction proceeds in the toluene- $^2\text{H}_2\text{O}$ system, trimethylammonium hydroxide eliminates from the toluene medium and under the reaction conditions it decomposes in an aqueous medium with the formation of trimethylamine and water. Thus, the final stage process may be described as proton abstraction from cation that results in the deactivation of a base. The proposed mechanism is also supported by the fact that an increase in the reaction time does not have a significant effect on the yield of **8**. The reaction between **7** and methyl 2-acetamidoacrylate in EtOH does not give the desired product. According to the proposed mechanism, in this case the proton abstraction from solvent by the enolate **A** forms an EtO^- anion, which is not eliminated from the reaction system. The EtO^- anion being formed may undergo the Michael addition reaction, as well as **7** and/or deboronate *o*-carborane structure. The explanation

above can be applied to a reaction in a system of two miscible liquids, such as THF-H₂O. The formed hydroxide anion remains in one system with the reactants to yield mainly a *nido*-carborane product.

5. Conclusions

Two possibilities of the sulfa-Michael addition reaction in the synthesis of *o*-carboranyl-DL-cysteine were investigated. The reaction proceeding between the trimethylammonium salt of 1-mercapto-*o*-carborane and methyl 2-acetamidoacrylate in the two-phase system, toluene-H₂O with base, as expected, demonstrates a low yield. Using the “free of base” method under the mild conditions in the two-phase system, the side processes were minimized and after the deprotection 1-HOOCCH(NH₂)CH₂S-1,2-C₂B₁₀H₁₁ was obtained in a good total yield. The developed “free of base” method was applied for the preparation of *o*-carboranyl-DL-cysteine labeled with deuterium at the α -position of amino acid using cheap and easily available ²H₂O as a deuterium source. The obtained compounds can be considered as potential agents for the Boron Neutron Capture Therapy of cancer as well as for protein metabolism studies.

Supplementary Materials: The following are available online at <http://www.mdpi.com/2073-4352/10/12/1133/s1>.

Author Contributions: Synthesis and writing—original draft preparation, J.L.; synthesis, M.S.; NMR research analysis, I.K.; X-ray diffraction study, I.A.; supervision, V.B. and I.S. All authors have read and agreed to the published version of the manuscript.

Funding: This work was supported by the Russian Science Foundation (№ 19-72-30005).

Acknowledgments: The NMR spectroscopy studies and X-ray diffraction experiment were performed using equipment of the Center for Molecular Structure Studies at A.N. Nesmeyanov Institute of Organoelement Compounds operating with financial support of the Ministry of Science and Higher Education of the Russian Federation.

Conflicts of Interest: The authors declare no conflict of interest.

References

1. Siegel, R.L.; Miller, K.D.; Jemal, A. Cancer statistics. *CA Cancer J. Clin.* **2019**, *69*, 7–34. [[CrossRef](#)] [[PubMed](#)]
2. Black, P.M. Brain Tumors. *N. Engl. J. Med.* **1991**, *324*, 1471–1476. [[CrossRef](#)] [[PubMed](#)]
3. Shah, H.K.; Mehta, M.P. Radiation Therapy. In *High-Grade Gliomas. Current Clinical Oncology*; Barnett, G.H., Ed.; Humana Press: Totowa, NJ, USA, 2007; pp. 231–244. [[CrossRef](#)]
4. Afseth, J.; Neubeck, L.; Karatzias, T.; Grant, R. Holistic needs assessment in brain cancer patients: A systematic review of available tools. *Eur. J. Cancer Care* **2018**, *28*, e12931. [[CrossRef](#)]
5. Locher, G.L. Biological effects and therapeutic possibilities of neutrons. *Am. J. Roentgenol. Radium Ther.* **1936**, *36*, 1–13.
6. Tolpin, E.I.; Wellum, G.R.; Dohan, F.C., Jr.; Komblith, P.R.; Zamenhof, R.G. Boron Neutron Capture Therapy of Cerebral Gliomas. *Oncology* **1975**, *32*, 223–246. [[CrossRef](#)] [[PubMed](#)]
7. Barth, R.F.; Zhang, Z.; Liu, T. A realistic appraisal of boron neutron capture therapy as a cancer treatment modality. *Cancer Commun.* **2018**, *38*, 36. [[CrossRef](#)] [[PubMed](#)]
8. Xuan, S.; Vicente, M.G.H. Recent Advances in Boron Delivery Agents for Boron Neutron Capture Therapy (BNCT). In *Boron-Based Compounds: Potential and Emerging Applications in Biomedicine*; Hey-Hawkins, E., Viñas, C., Eds.; John Wiley & Sons: Hoboken, NJ, USA, 2018; pp. 298–342.
9. Henriksson, R.; Capala, J.; Michanek, A.; Lindahl, S.-Å.; Salford, L.G.; Franzén, L.; Blomquist, E.; Westlin, J.-E.; Bergenheim, T.A. Boron Neutron Capture Therapy (BNCT) for Glioblastoma Multiforme: A Phase II Study Evaluating A Prolonged High-Dose of Boronophenylalanine (BPA). *Radiother. Oncol.* **2008**, *88*, 183–191. [[CrossRef](#)]
10. Kulvik, M.; Vähätalo, J.; Buchar, E.; Färkkilä, M.; Järviluoma, E.; Jääskeläinen, J.; Křiž, O.; Laakso, J.; Rasilainen, M.; Ruokonen, I.; et al. Clinical implementation of 4-dihydroxyborylphenylalanine synthesised by an asymmetric pathway. *Eur. J. Pharm. Sci.* **2003**, *18*, 155–163. [[CrossRef](#)]
11. Barth, R.F.; Coderre, J.F.; Vicente, M.G.H.; Blue, T.E. Boron Neutron Capture Therapy of Cancer: Current Status and Future Prospects. *Clin. Cancer Res.* **2005**, *11*, 3987–4002. [[CrossRef](#)]

12. Hu, K.; Yang, Z.; Zhang, L.; Xie, L.; Wang, L.; Xu, H.; Josephson, L.; Liang, S.H.; Zhang, M.-R. Boron agents for neutron capture therapy. *Coord. Chem. Rev.* **2020**, *405*, 213139. [[CrossRef](#)]
13. Kabalka, G.W.; Yao, M.-L. The synthesis and use of boronated amino acids for boron neutron capture therapy. *Anticancer Agents Med. Chem.* **2006**, *6*, 111–125. [[CrossRef](#)] [[PubMed](#)]
14. Hawthorne, M.F. The Role of Chemistry in the Development of Boron Neutron Capture Therapy of Cancer. *Angew. Chem. Int. Ed. Engl.* **1993**, *32*, 950–984. [[CrossRef](#)]
15. Sivaev, I.B.; Bregadze, V.I. Polyhedral Boranes for Medical Applications: Current Status and Perspectives. *Eur. J. Inorg. Chem.* **2009**, 1433–1450. [[CrossRef](#)]
16. Grimes, R.N. *Carboranes*, 3rd ed.; Academic Press: New York, NY, USA; Elsevier: Amsterdam, The Netherlands, 2016.
17. Stogniy, M.Y.; Zakharova, M.V.; Sivaev, I.B.; Godovikov, I.A.; Chizov, A.O.; Bregadze, V.I. Synthesis of new carborane-based amino acids. *Polyhedron* **2013**, *55*, 117–120. [[CrossRef](#)]
18. Leukart, O.; Caviezel, M.; Eberle, A.; Escher, E.; Tun-Kyi, A.; Schwyzer, R. L-o-Carboranylalanine, a Boron Analogue of Phenylalanine. *Helv. Chim. Acta* **1976**, *59*, 2184–2187. [[CrossRef](#)]
19. Gruzdev, D.A.; Levit, G.L.; Olshevskaya, V.A.; Krasnov, V.P. Synthesis of ortho-Carboranyl Derivatives of (S)-Asparagine and (S)-Glutamine. *Russ. J. Org. Chem.* **2017**, *5*, 769–776. [[CrossRef](#)]
20. Prashar, J.K.; Moore, D.E. Synthesis of Carboranyl Phenylalanine for Potential Use in Neutron Capture Therapy of Melanoma. *J. Chem. Soc. Perkin Trans. 1* **1993**, 1051–1053. [[CrossRef](#)]
21. Gruzdev, D.A.; Ustinov, V.O.; Levit, G.L.; Ol'shevskaya, V.A.; Krasnov, V.P. Synthesis of meta-Carboranyl-(S)-homocysteine Sulfoxide. *Russ. J. Org. Chem.* **2018**, *54*, 1579–1582. [[CrossRef](#)]
22. He, T.; Misuraca, J.C.; Musah, R.A. "Carboranyl-Cysteine"-Synthesis, Structure and Self-Assembly Behavior of a Novel α -Amino Acid. *Sci. Rep.* **2017**, *7*, 16995. [[CrossRef](#)]
23. He, T.; Musah, R.A. Evaluation of the Potential of 2-Amino-3-(1,7-dicarba-closododecaboranyl-1-thio)propanoic Acid as a Boron Neutron Capture Therapy Agent. *ACS Omega* **2019**, *4*, 3820–3826. [[CrossRef](#)]
24. He, T.; Chittur, S.V.; Musah, R.A. Impact on Glioblastoma U87 Cell Gene Expression of a Carborane Cluster bearing Amino Acid: Implications for Carborane Toxicity in Mammalian Cells. *ACS Chem. Neurosci.* **2019**, *10*, 1524–1534. [[CrossRef](#)] [[PubMed](#)]
25. Vinas, C.; Benakki, R.; Teixidor, F.; Casabo, J. Dimethoxyethane as a Solvent for the Synthesis of C-Monosubstituted o-Carborane Derivatives. *Inorg. Chem.* **1995**, *34*, 3844–3845. [[CrossRef](#)]
26. Plešek, J.; Heřmanek, S. Syntheses and properties of substituted icosahedral carborane thiols. *Collect. Czech. Chem. Commun.* **1981**, *46*, 687–692. [[CrossRef](#)]
27. Stogniy, M.Y.; Erokhina, S.A.; Druzina, A.A.; Sivaev, I.B.; Bregadze, V.I. Synthesis of novel carboranyl azides and "click" reactions thereof. *J. Organomet. Chem.* **2019**, *904*, 121007. [[CrossRef](#)]
28. Frisch, M.J.; Trucks, G.W.; Schlegel, H.B.; Scuseria, G.E.; Robb, M.A.; Cheeseman, J.R.; Scalmani, G.; Barone, V.; Petersson, G.A.; Nakatsuji, H.; et al. *Gaussian 09, Revision, D.01*; Gaussian, Inc.: Wallingford, CT, USA, 2016.
29. Perdew, J.; Ernzerhof, M.; Burke, K. Rationale for mixing exact exchange with density functional approximations. *J. Chem. Phys.* **1996**, *105*, 9982–9985. [[CrossRef](#)]
30. Carlo, A.; Barone, V. Toward reliable density functional methods without adjustable parameters: The PBE0 model. *J. Chem. Phys.* **1999**, *110*, 6158–6170. [[CrossRef](#)]
31. Keith, T.A. *TK Gristmill Software*; AIMAll (Version 19.10.12): Overland Park, KS, USA, 2019.
32. Cossec, B.; Cosnier, F.; Burgart, M. Methyl Mercapturate Synthesis: An Efficient, Convenient and Simple Method. *Molecules* **2008**, *13*, 2394–2407. [[CrossRef](#)]
33. Davidson, M.G.; Fox, M.A.; Hibbert, T.G.; Howard, J.A.K.; Mackinnon, A.; Neretin, I.S.; Wade, K. Deboronation of orthocarborane by an iminophosphorane: Crystal structures of the novel carborane adduct nido-C₂B₁₀H₁₂·HNP(NMe₂)₃ and the borenium salt [(Me₂N)₃PNHBNP(NMe₂)₃]₂O₂⁺ (C₂B₉H₁₂⁻)₂. *Chem. Commun.* **1999**, 1649–1650. [[CrossRef](#)]
34. Svantesson, E.; Pettersson, J.; Olin, Å.; Markides, K.E. A kinetic study of the self-degradation of o-carboranylalanine to nido-carboranylalanine in solution. *Acta Chem. Scand.* **1999**, *53*, 731–736. [[CrossRef](#)]
35. Taoda, Y.; Sawabe, T.; Endo, Y.; Yamaguchi, K.; Fujii, S.; Kagechika, H. Identification of an intermediate in the deboronation of ortho-carborane: An adduct of ortho-carborane with two nucleophiles on one boron atom. *Chem. Commun.* **2008**, 2049–2051. [[CrossRef](#)]

36. Kononov, L.O.; Orlova, A.V.; Zinin, A.I.; Kimel, B.G.; Sivaev, I.B.; Bregadze, V.I. Conjugates of polyhedral boron compounds with carbohydrates. 2. Unexpected easy *closo*- to *nido*-transformation of a carborane–carbohydrate conjugate in neutral aqueous solution. *J. Organomet. Chem.* **2005**, *690*, 2769–2774. [[CrossRef](#)]
37. Likhoshesterov, L.M.; Novikova, O.S.; Chizhov, A.O.; Sivaev, I.B.; Bregadze, V.I. Conjugates of polyhedral boron compounds with carbohydrates 8. Synthesis and properties of *nido-ortho*-carborane glyco conjugates containing one to three β -lactosylamine residues. *Russ. Chem. Bull.* **2011**, *60*, 2359–2364. [[CrossRef](#)]
38. Núñez, R.; Teixidor, F.; Kivekäs, R.; Sillanpää, R.; Viñas, C. Influence of the solvent and R groups on the structure of (carboranyl) R_2PI_2 compounds in solution. Crystal structure of the first iodophosphonium salt incorporating the anion $[7,8\text{-nido-C}_2\text{B}_9\text{H}_{10}]^-$. *Dalton Trans.* **2008**, 1471–1480. [[CrossRef](#)]
39. Teixidor, F.; Viñas, C.; Mar Abad, M.; Nuñez, R.; Sillanpää, R. Procedure for the degradation of 1,2-(PR₂)₂-1,2-dicarba-*closo*-dodecaborane(12) and 1-(PR₂)-2-R'-1,2-dicarba-*closo*-dodecaborane(12). *J. Organomet. Chem.* **1995**, *503*, 193–203. [[CrossRef](#)]
40. Poater, J.; Viñas, C.; Bennour, I.; Escayola, S.; Solà, M.; Teixidor, F. Too Persistent to Give up: Aromaticity in Boron Clusters Survives Radical Structural Changes. *J. Am. Chem. Soc.* **2020**, *142*. [[CrossRef](#)] [[PubMed](#)]
41. Boyd, L.A.; Clegg, W.; Copley, R.C.B.; Davidson, M.G.; Fox, M.A.; Hibbert, T.G.; Howard, J.A.; Mackinnon, K.A.; Peace, R.J.; Wade, K. Exo- π -bonding to an *ortho*-carborane hypercarbon atom: Systematic icosahedral cage distortions reflected in the structures of the fluoro-, hydroxy- and amino-carboranes, 1-X-2-Ph-1,2-C₂B₁₀H₁₀ (X = F, OH or NH₂) and related anions. *Dalton Trans.* **2004**, 2786–2799. [[CrossRef](#)] [[PubMed](#)]
42. Stogniy, M.Y.; Sivaev, I.B.; Petrovskii, P.V.; Bregadze, V.I. Synthesis of monosubstituted functional derivatives of carboranes from 1-mercapto-*ortho*-carborane: 1-HOOC(CH₂)_nS-1,2-C₂B₁₀H₁₁ and $[7\text{-HOOC(CH}_2\text{)}_n\text{S-7,8-C}_2\text{B}_9\text{H}_{11}]^-$ (n = 1–4). *Dalton Trans.* **2010**, *39*, 1817–1822. [[CrossRef](#)]
43. Romanova, A.; Lyssenko, K.; Ananyev, I. Estimations of energy of noncovalent bonding from integrals over interatomic zero-flux surfaces: Correlation trends and beyond. *J. Comput. Chem.* **2018**, *39*, 1607–1616. [[CrossRef](#)]
44. Mutlib, A.E. Application of Stable Isotope-Labeled Compounds in Metabolism and in Metabolism-Mediated Toxicity Studies. *Chem. Res. Toxicol.* **2008**, *21*, 1672–1689. [[CrossRef](#)]
45. Wilkinson, D.J. Historical and contemporary stable isotope tracer approaches to studying mammalian protein metabolism. *Mass Spectrom. Rev.* **2018**, *37*, 57–80. [[CrossRef](#)]
46. Pająk, M.; Pałka, K.; Winnicka, E.; Kańska, M. The chemo- enzymatic synthesis of labeled l-amino acids and some of their derivatives. *J. Radioanal. Nucl. Chem.* **2018**, *317*, 643–666. [[CrossRef](#)] [[PubMed](#)]

Publisher’s Note: MDPI stays neutral with regard to jurisdictional claims in published maps and institutional affiliations.



© 2020 by the authors. Licensee MDPI, Basel, Switzerland. This article is an open access article distributed under the terms and conditions of the Creative Commons Attribution (CC BY) license (<http://creativecommons.org/licenses/by/4.0/>).